42nd AIAA/ASME/SAE/ASEE Joint Propulsion Conference & Exhibit
9 - 12 July 2006, Sacramento, California

AIAA 2006-5157

Operation of a Coaxial High Energy (CHENG) Thruster

Flavio Poehlmann[1], Nicolas Gascon[2], Cliff Thomas[3], and Mark Cappelli[4]
Stanford University, Stanford, CA, 94305

The Coaxial High ENerGy (CHENG) Thruster is a high power coaxial pulsed plasma accelerator that was first proposed in 1970 by D.Y. Cheng. Reported exhaust velocities on the order of 10^6m/s, thrust densities on the order of 10^5N/m^2 and low erosion rates make this thruster attractive for a variety of space missions. However, little work has been published since 1970 and the acceleration mechanism is not well understood. Therefore, the concept was recently reintroduced to the electric propulsion community with the goal of building scaled down versions that can operate at lower energy levels and higher pulse rates. This paper gives an overview of the design of a 3kJ CHENG thruster and first experimental results from its operation.

Nomenclature

B	=	magnetic field
$C_{C\text{-}J}$	=	electromagnetic Chapman-Jouguet speed
c_{sound}	=	speed of sound
e	=	internal energy
H	=	Hugoniot constant
h	=	enthalpy
L	=	energy lost
p	=	pressure
q	=	energy input
u	=	velocity of plasma fluid
γ	=	specific heat ratio
μ_0	=	permeability constant
ν_A	=	Alfven velocity
ρ	=	density

I. Introduction

THE Coaxial High ENerGy (CHENG) Thruster is a high power, high density, pulsed coaxial plasma accelerator. It was first studied in the late 1960s by Cheng[1,3], but little theoretical or experimental data is available since 1970. In its most general configuration, it was operated at 20,000 Volts and discharged 12kJ of stored electrical energy during a 10μs pulse to accelerate a dense 10^{15}cm^{-3} hydrogen or argon plasma to exhaust velocities on the order of 10^6m/s. Motivated by reported high thrust density, high efficiency and low electrode erosion rates, the Stanford Plasma Dynamics Lab has recently reintroduced the concept[2]. The goal is to build scaled down versions of the thruster that can operate at similarly high number densities but at lower energy levels, higher pulse rates and a specific impulse one or two orders of magnitude lower. The CHENG thruster could then be a viable option for high power high thrust applications and thus a solution to the long standing problem of high electrode erosion rates in this operating regime. However, despite promising experimental data, the physics governing the plasma acceleration mechanism are not well understood. Therefore extensive numerical and experimental studies are required to optimize thruster operation and enable proper scaling of the relevant operating parameters. As a first step, a CHENG thruster is currently being developed that can process an energy of 3kJ over a 10μs pulse at an applied potential of

[1] Research Assistant, Mechanical Engineering, Building 520, AIAA Student Member.
[2] Research Associate, Mechanical Engineering, Building 520, AIAA Member.
[3] Research Assistant, Mechanical Engineering, Building 520, AIAA Student Member.
[4] Professor, Mechanical Engineering, Building 520, AIAA Member.

8kV. This paper summarizes the current status of this project and describes design considerations, as well as some preliminary experimental results.

Figure 1 shows a schematic of the Stanford 3kJ CHENG thruster. This version is designed to be operated with seven 15μF capacitors, which are permanently connected to the thruster electrodes. No switch is required since the thruster is in vacuum. Therefore, electrical breakdown between the thruster electrodes is initially held off on the vacuum side of the Paschen curve. After charging the capacitors, the discharge is initiated by a puff of argon gas that is injected at the breach of the thruster through a fast acting valve which opens and closes on the order of a few microseconds. Upon entering the co-axial channel, rapid avalanche ionization causes the gas to immediately break down. The resulting current then induces an azimuthal magnetic field, and the combination of thermal heating and electromagnetic force accelerates the plasma to very high exhaust velocities. A particular advantage of this mode of operation is that the valve acts as the switch that initiates and terminates the discharge pulse. This helps efficient propellant utilization and keeps the control circuitry relatively simple.

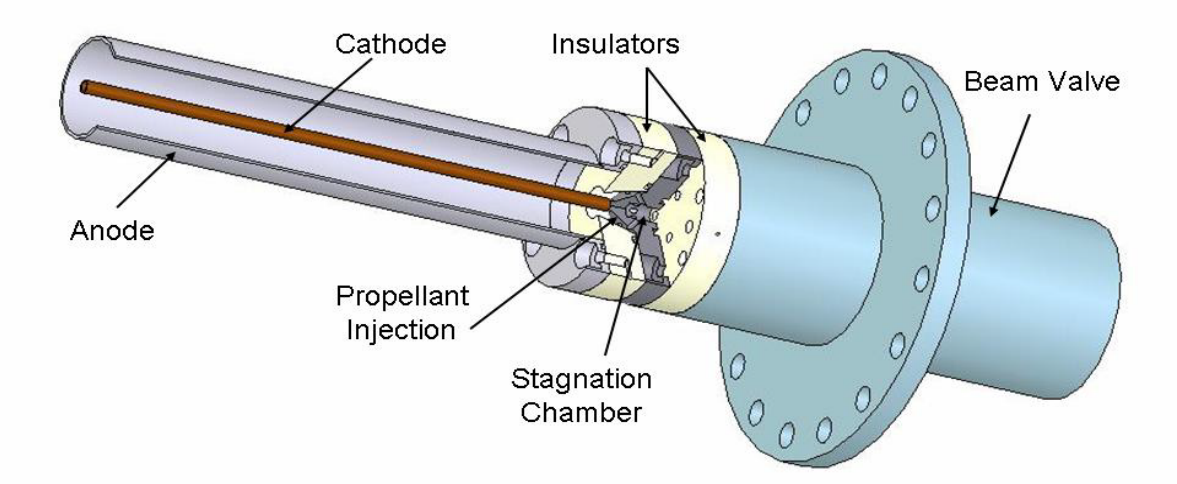

Figure 1. Schematic diagram of the Stanford 3kJ CHENG thruster.

The remaining sections of this paper are organized as follows. First a brief overview is given of existing theoretical and numerical models of the plasma acceleration mechanism. Then the thruster and the power processing system are described. Finally, preliminary findings from a first firing of the thruster are presented.

II. Existing Theory

The only theoretical description of this co-axial discharge that is published in the open literature is that presented by Cheng[1,3] and Watson[4]. An extensive summary of these existing theoretical and numerical models was published in a previous paper[2]. Therefore this section only provides a brief review.

Figure 2 shows a schematic of the acceleration region inside the thruster. As the neutral particles enter the electrode gap they immediately break down in a thin ionization region (zone 1). The resulting current heats the gas and leads to thermal expansion. In addition, the self-induced magnetic field pointing into the page causes the plasma to drift downstream. This heating and expansion region (zone 2) transitions into a collisionless acceleration region (zone 3). In this region the high particle speeds have led to sufficient reduction in density and cross-sectional area for Coulomb collisions so that the plasma can be treated as collisionless.

A. Heating and Expansion Region

Cheng compares the heating and expansion region to a deflagration and uses a fluid description to draw an analogy to the Rankine-Hugoniot theory in chemical combustion theory[1]. Accounting for magnetic pressure and magnetic energy he writes the conservation equations for mass, momentum and energy across zone 2:

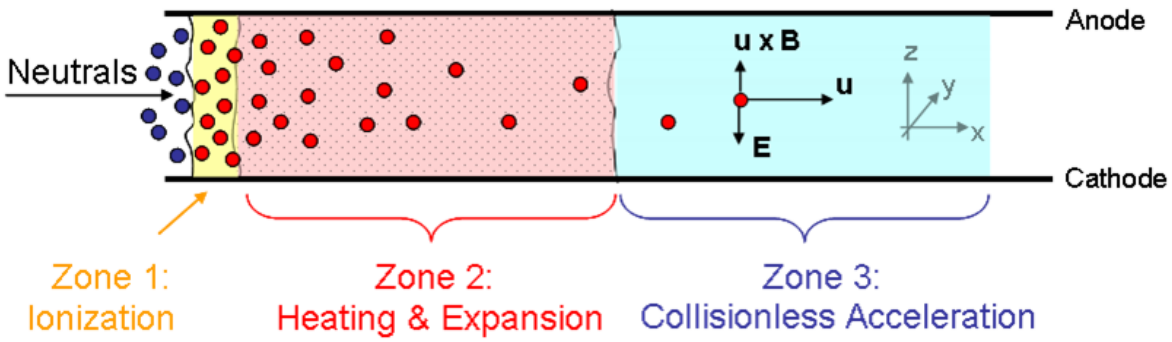

Figure 2. Acceleration region of the CHENG thruster.

$$\rho_1 u_1 = \rho_3 u_3 \tag{1}$$

$$\rho_1 u_1^{\,2} + p_1 + \frac{B_1^{\,2}}{2\mu_0} = \rho_3 u_3^{\,2} + p_3 + \frac{B_3^{\,2}}{2\mu_0} \tag{2}$$

$$h_1 + \frac{1}{2}u_1^{\,2} + \frac{B_1^{\,2}}{2\rho_1\mu_0} + q = h_3 + \frac{1}{2}u_3^{\,2} + \frac{B_3^{\,2}}{2\rho_3\mu_0} + L \tag{3}$$

After introducing the total pressure p* as the sum of dynamic and magnetic pressure and an equivalent specific energy e* given by

$$p^* = p + \frac{B^2}{2\mu_0} \tag{4}$$

$$e^* = e + \frac{B^2}{2\mu_0\rho} \tag{5}$$

the equations of motion reduce to the same form that is used to derive the Rankine-Hugoniot relationship in combustion theory. However, the equivalent Chapman-Jouguet speed $C_{C\text{-}J}$ for the plasma deflagration case is given by the sum of squares of the Alfven speed and sound speed.

$$C_{C-J} = \sqrt{\gamma\frac{p_1}{\rho_1} + \frac{B_1^{\,2}}{\rho_1\mu_0}} = \sqrt{c_{sound}^{\,2} + v_A^{\,2}} \tag{6}$$

A similar description of a plasma deflagration can also be found in the book by Sutton[5]. Cheng argues that the thruster operates in a thermally choked plasma deflagration mode. For this case the velocity of the processed plasma at the end of zone 2 is $C_{C\text{-}J}$ and thus is of an order of magnitude that is consistent with experimental data. Operation in a thermally choked deflagration mode also explains the low observed electrode erosion rate as deflagration waves are "thick" and thus reduce current density on the electrodes. It also explains the high exhaust velocities as deflagration waves are very efficient at converting added energy to directed kinetic rather than thermal energy.

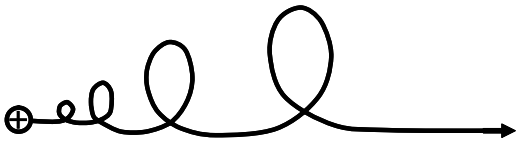

Figure 3. Representative ion motion in the collisionless acceleration region of the CHENG thruster.

B. Collisionless Acceleration Region

After leaving the thermal heating and expansion region, the plasma enters the collisionless acceleration region. Particle in cell simulations by Watson *et al*[4] and more recently by Poehlmann *et al*[2] show that in the collisionless acceleration region the fully magnetized ions drift through a negative magnetic pressure gradient. During this drifting motion, the Larmor radius increases until the ions are released from their cyclotron orbits. As the ions move downstream and into regions of weaker magnetic field, the magnitude of the $\mathbf{u}\times\mathbf{B}$ force, which is directed radially outward, approaches that of the electrostatic force, which is directed radially inward. In the limiting case, these two forces balance and the ion moves downstream in a straight path. This is illustrated in Fig. 2 and 3.

III. Design of the Thruster and Power Processing Unit

The CHENG thruster system consists of three main components: (i) the thruster, (ii) the electric power circuit and (iii) the beam valve.

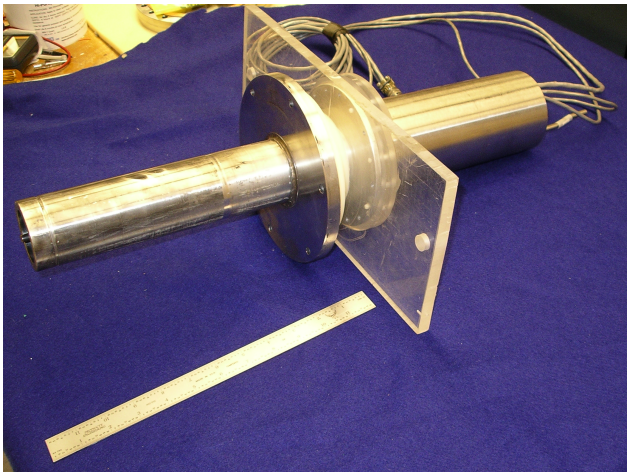

Figure 4. The Stanford 3kJ CHENG thruster.

Figure 5. Power processing unit for the Stanford 3kJ CHENG thruster.

A. Thruster

Figure 4 shows a photograph of Stanford's 3 kJ CHENG thruster. Its general design was described in section I. The anode is made of stainless steel, is 9.5 inches long and has an inner diameter of 1.75 inches. The cathode is made of copper and has an outer radius of 0.25 inches. The stagnation chamber shown in Fig. 1 was reproduced from Cheng's original designs. The exact significance of the stagnation chamber at the base of the cathode has not been studied yet. However, according to Cheng it serves to ensure that the gas enters the electrode gap with a uniform front[1].

B. Power Processing System

Figure 5 shows a photograph of the power processing system. A General Atomics CCS power supply that can provide 12kW and 10kV at a steady state charging current of 2.4A is used to charge the capacitors. When the capacitors are discharged during thruster operation the possibility of voltage reversal exists across the capacitor bank due to finite inductance in the system. Such voltage reversal is harmful to the capacitors and especially to the power supply. Therefore, a protective circuit was designed around a CKE high voltage diode stack CJV06H-S to protect the power supply. This protective circuit and four of the seven capacitors are shown on the right hand side of Fig. 5. The circuit diagram is shown in Fig. 6. The high voltage diode stack D shorts the circuit for the case of reversed voltage across the capacitors so that potentially hazardous energy can be dissipated by the resistor R2=25Ω. During this process the power supply is isolated from the protective circuit by the resistor R1=25Ω. If the thruster is operated in single shot mode, switch S1 can be used as an added safety feature to disconnect the power supply from the capacitor bank while firing the thruster. In case of a thruster malfunction or if the firing needs to be aborted after the capacitors have already been charged, switch S2 can be used to safely discharge the capacitor bank through the resistor bank R3=2,000Ω.

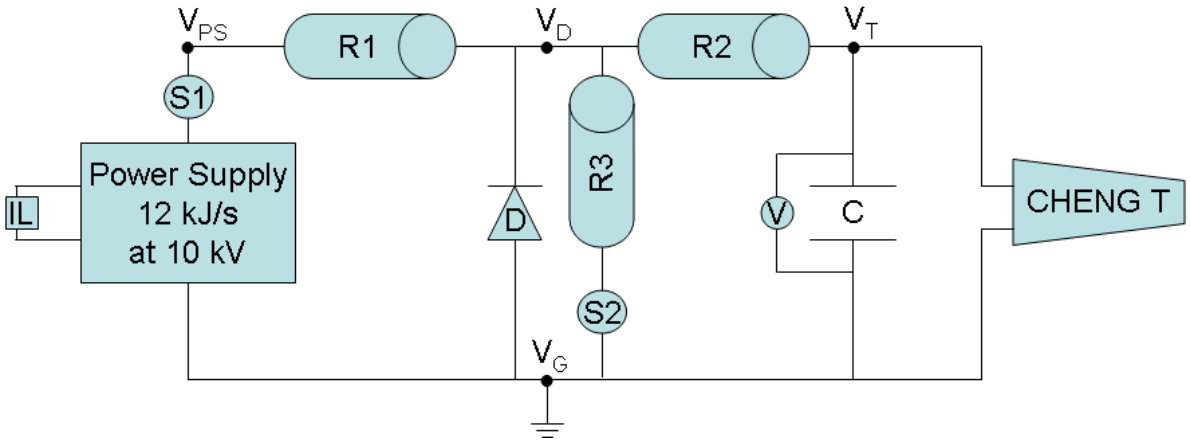

Figure 6. Circuit diagram for the power supply protective circuit.

C. Beam Valve

A crucial component for the operation of the thruster is the propellant valve. It has to be able to deliver a peak mass flow rate on the order of 1 g/s over a timeframe of just a few microseconds. These requirements are met by the Jordan C-211 Pulsed Beam Valve, which can be seen on the right hand side of Fig.4. This valve employs the magnetic beam repulsion principle illustrated in Fig. 7. If a high current is passed through the beam conductor, the generated magnetic force causes the top beam to be lifted from the O-ring seal over the nozzle, allowing gas to flow through it. The user can apply a back pressure of up to 10 atm to ensure choked flow and use nozzles with diameters between 0.1 and 1 millimeter. Therefore, mass flow rates on the order of 1 g/s and lower can be achieved. Depending on the amount of current that is passed through the beam conductors, the pulse width of the gas should be around 20 μs. The pulse width can be measured using a fast ionization gauge.

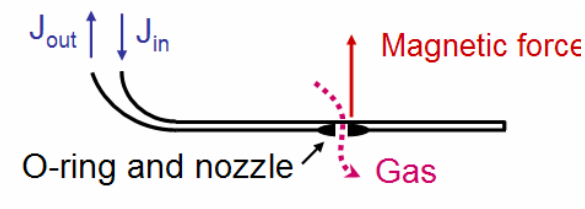

Figure 7: Magnetic beam repulsion principle used in the fast pulsed beam valve.

IV. Results

Figure 8 shows the experimental setup for the first operation of the Stanford 3kJ Cheng thruster. The thruster was horizontally mounted on the right side of the vacuum chamber and two plasma potential probes spaced 12 inches apart were placed in the path of the plasma exhaust stream. The time delay between the two probes was used to measure time of flight and thus provide a first order estimate of the exhaust velocity. At this stage, only four of the seven capacitors were used and the thruster was operated at 4,000 instead of 8,000 Volts. Therefore, the energy per pulse was 480J. The valve was set to deliver approximately 1μg of argon gas per pulse.

The thruster was fired at a rate of 1Hz and the discharge was recorded using a standard digital camera. Since the minimum exposure time of the camera was limited to 1ms and thus several orders of magnitude higher than the characteristic time scales of the discharge, only one frame was obtained per pulse and this frame shows a time integrated image of the discharge. A representative image of a discharge pulse is shown in Fig. 9 and depicts clearly the ejection of a plasma beam from the thruster. Both plasma probes saturated approximately 2μs into the pulse but suggested a plasma velocity on the order of 10^4 - 10^5 m/s. However, the image also illustrates that the plasma beam is not perfectly focused and diverges rather quickly. In addition, some plasma leaked onto the outer surface of the anode. This suggests that the thruster may not yet be operating in the efficient mode described in the early studies of Cheng. This was expected since the stored energy and applied voltage for the first test were significantly lower than the values for which it was designed.

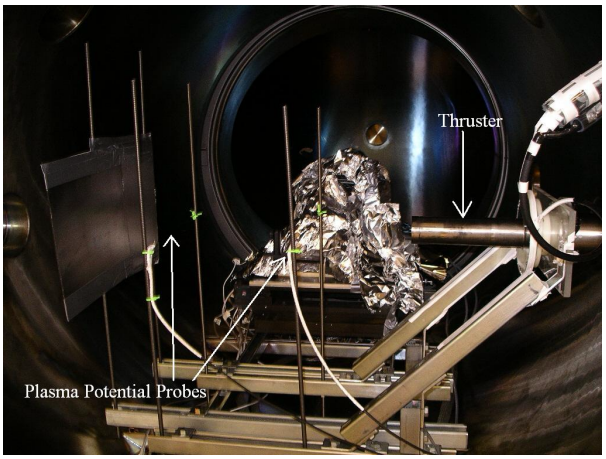

Figure 8. Experimental setup of CHENG thruster and plasma probes.

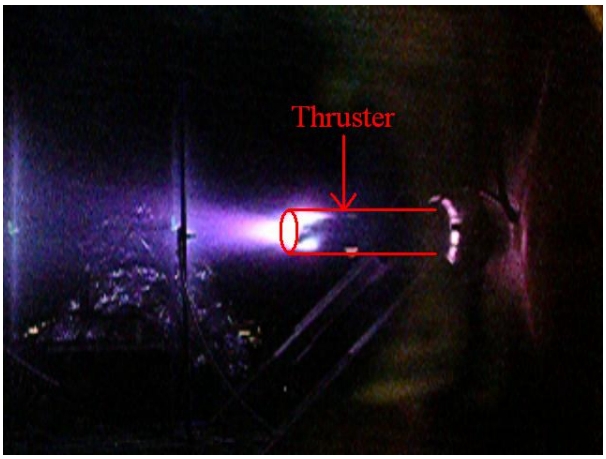

Figure 9. CHENG thruster discharge at 4kV and 480J.

As the frequency was increased to 5 Hz, the high voltage coaxial cable inside the chamber overheated and melted. This suggests that radiative cooling is not sufficient at higher operating frequencies and it may be necessary to water cool the power lines running into the chamber and to the thruster. In addition, special attention needs to be paid to proper insulation of all conducting surfaces as the high electric and magnetic field variations occur on the order of microseconds and can thus lead to stray discharges.

V. Conclusion

A 3kJ CHENG thruster and accompanying power processing system were designed and successfully tested in the laboratory. A discharge was attained, but since the operating voltage and pulse energy were significantly lower than its design parameters, the preliminary results cannot yet be used for a full validation of the thruster concept. Nevertheless, the preliminary results are promising and identify future work. The next steps include using all seven capacitors and increasing the operating voltage to 8,000V. Diagnostic techniques will have to be developed to measure thruster performance.

Acknowledgments

The authors would like to extend their appreciation to Prof. D.Y. Cheng, for the many stimulating discussions, the donation of valuable equipment, and for introducing us to this interesting propulsion concept. We would also like to acknowledge Dr. Jean-Luc Cambier (AFRL) for providing the needed power supplies and access to the OOPIC code, and Dr. William Hargus (AFRL) for some fabricated thruster components. Finally, we would like to thank Paul Shoessow, John Cary, Ammar Hakim and Peter Stoltz at Tech-Ex, for guidance in carrying out the OOPIC simulations, and our colleague Ms. Emmanuelle Sommier for assistance in the fabrication of the Stanford thruster.

References

[1]Cheng, D.Y., "*Plasma Deflagration and the Properties of a Coaxial Plasma Deflagration Gun*", Nuclear Fusion 10, 1970

[2]Poehlmann, F., Gascon, N., Thomas, C., Cappelli, M., *"The Coaxial High Energy Thruster"*, International Electric Propulsion Conference, IEPC-2005-100, October 2005

[3]Cheng, D.Y., "*Application of a Deflagration Plasma Gun as a Space Propulsion Thruster*", AIAA Journal Vol.9, No.9, September 1971

[4]Watson, V.R., "*Computer Simulation of a Plasma Accelerator*", Ph.D. Dissertation, Stanford University, 1969

[5]Sutton, G.W., Sherman, A., *"Engineering Magnetohydrodynamics"*, McGraw-Hill, 1965